



Resting state EEG power spectrum and functional connectivity in autism: a cross-sectional analysis

Pilar Garcés, Sarah Baumeister, Luke Mason, Christopher Chatham, Stefan Holiga, Juergen Dukart, Emily Jones, Tobias Banaschewski, Simon Baron-Cohen, Sven Bölte, et al.

► To cite this version:

Pilar Garcés, Sarah Baumeister, Luke Mason, Christopher Chatham, Stefan Holiga, et al.. Resting state EEG power spectrum and functional connectivity in autism: a cross-sectional analysis. *Molecular Autism*, 2022, 13 (1), pp.22. 10.1186/s13229-022-00500-x . pasteur-04072081

HAL Id: pasteur-04072081

<https://pasteur.hal.science/pasteur-04072081>

Submitted on 17 Apr 2023

HAL is a multi-disciplinary open access archive for the deposit and dissemination of scientific research documents, whether they are published or not. The documents may come from teaching and research institutions in France or abroad, or from public or private research centers.

L'archive ouverte pluridisciplinaire **HAL**, est destinée au dépôt et à la diffusion de documents scientifiques de niveau recherche, publiés ou non, émanant des établissements d'enseignement et de recherche français ou étrangers, des laboratoires publics ou privés.



Distributed under a Creative Commons Attribution 4.0 International License

RESEARCH

Open Access



Resting state EEG power spectrum and functional connectivity in autism: a cross-sectional analysis

Pilar Garcés^{1*} , Sarah Baumeister², Luke Mason³, Christopher H. Chatham¹, Stefan Holiga¹, Juergen Dukart^{4,5}, Emily J. H. Jones³, Tobias Banaschewski², Simon Baron-Cohen⁶, Sven Bölte^{7,8}, Jan K. Buitelaar⁹, Sarah Durston¹⁰, Bob Oranje¹⁰, Antonio M. Persico¹¹, Christian F. Beckmann⁹, Thomas Bougeron¹², Flavio Dell'Acqua¹³, Christine Ecker^{13,14}, Carolin Moessnang², Tony Charman¹³, Julian Tillmann¹, Declan G. M. Murphy¹³, Mark Johnson³, Eva Loth¹³, Daniel Brandeis^{2,15,16}, Joerg F. Hipp¹ and The EU-AIMS LEAP group authorship

Abstract

Background: Understanding the development of the neuronal circuitry underlying autism spectrum disorder (ASD) is critical to shed light into its etiology and for the development of treatment options. Resting state EEG provides a window into spontaneous local and long-range neuronal synchronization and has been investigated in many ASD studies, but results are inconsistent. Unbiased investigation in large and comprehensive samples focusing on replicability is needed.

Methods: We quantified resting state EEG alpha peak metrics, power spectrum (PS, 2–32 Hz) and functional connectivity (FC) in 411 children, adolescents and adults ($n = 212$ ASD, $n = 199$ neurotypicals [NT], all with $IQ > 75$). We performed analyses in source-space using individual head models derived from the participants' MRIs. We tested for differences in mean and variance between the ASD and NT groups for both PS and FC using linear mixed effects models accounting for age, sex, IQ and site effects. Then, we used machine learning to assess whether a multivariate combination of EEG features could better separate ASD and NT participants. All analyses were embedded within a train-validation approach (70%–30% split).

Results: In the training dataset, we found an interaction between age and group for the reactivity to eye opening ($p = .042$ uncorrected), and a significant but weak multivariate ASD vs. NT classification performance for PS and FC (sensitivity 0.52–0.62, specificity 0.59–0.73). None of these findings replicated significantly in the validation dataset, although the effect size in the validation dataset overlapped with the prediction interval from the training dataset.

Limitations: The statistical power to detect weak effects—of the magnitude of those found in the training dataset—in the validation dataset is small, and we cannot fully conclude on the reproducibility of the training dataset's effects.

Conclusions: This suggests that PS and FC values in ASD and NT have a strong overlap, and that differences between both groups (in both mean and variance) have, at best, a small effect size. Larger studies would be needed to investigate and replicate such potential effects.

*Correspondence: pilar.garces@roche.com

¹ Roche Pharma Research and Early Development, Neuroscience and Rare Diseases, Roche Innovation Center Basel, Basel, Switzerland
Full list of author information is available at the end of the article



© The Author(s) 2022. **Open Access** This article is licensed under a Creative Commons Attribution 4.0 International License, which permits use, sharing, adaptation, distribution and reproduction in any medium or format, as long as you give appropriate credit to the original author(s) and the source, provide a link to the Creative Commons licence, and indicate if changes were made. The images or other third party material in this article are included in the article's Creative Commons licence, unless indicated otherwise in a credit line to the material. If material is not included in the article's Creative Commons licence and your intended use is not permitted by statutory regulation or exceeds the permitted use, you will need to obtain permission directly from the copyright holder. To view a copy of this licence, visit <http://creativecommons.org/licenses/by/4.0/>. The Creative Commons Public Domain Dedication waiver (<http://creativecommons.org/publicdomain/zero/1.0/>) applies to the data made available in this article, unless otherwise stated in a credit line to the data.

Keywords: Autism spectrum disorder, EEG, Resting state, Power spectrum, Functional connectivity

Background

Autism spectrum disorder (ASD) is a prevalent neurodevelopmental condition, affecting around 1 in 54 children [1]. It is diagnosed in the presence of alterations in social communication, social interaction and restricted and repetitive behaviors and interests [2]. ASD is heterogeneous with diverse clinical presentations and frequent comorbidities including epilepsy, attention-deficit/hyperactivity disorder, anxiety and depression [3]. Currently, the pathophysiology of ASD is unclear. In particular, neuronal mechanisms underlying idiopathic ASD remain largely unknown [2]. Establishing potential differences in brain activity between ASD and NT and heterogeneities within the ASD population would be an important step to shed light into the etiology of the condition and facilitate the development of interventions.

Electrophysiological techniques such as EEG (electroencephalography) or MEG (magnetoencephalography) are suited to investigate macroscopic neuronal circuit function and maturation. They are noninvasive and direct measures of neuronal activity with a high temporal resolution enabling the evaluation of brain dynamics and brain rhythms. The value of EEG in ASD was recently highlighted by several investigations showing a consistent deviation of event-related activity in response to presentation of human faces [4], i.e., the N170 latency, and subsequent efforts to develop it into a qualified biomarker for use in ASD clinical trials [5]. Besides the event-locked EEG response to sensory stimuli, resting state EEG—that is the EEG signal in the absence of any specific task—could provide important insights into brain circuitry associated with ASD. In particular, the resting state power spectrum (PS), quantifying local synchronization within brain regions, and functional connectivity (FC) measures, quantifying long-range interactions between distant brain areas, are key characteristics of the resting-state EEG [6, 7].

Many studies have evaluated resting state EEG/MEG PS and FC in ASD across brain rhythms, from the delta to the gamma range, and some focusing on the most prominent resting state rhythm: alpha. However, no clear picture has emerged yet. Various theories for PS alterations in ASD have been put forward, including a U-shaped profile with excessive power in low and high frequencies [8], but many findings are in conflict to each other. For example, for spectral power in the alpha band, there are various reports of increase [9–11], decrease [12–14] and no effects [15, 16] in ASD compared to NT (neurotypicals). O'Reilly et al. performed a systematic review of the FC

ASD literature [17]. Although a meta-analysis could not be performed due to large variability in methodology and samples across the 52 reports included, the authors concluded that there was a trend for a decrease of long-range FC in ASD—even as the frequency bands and brain/scalp regions of these effects were unclear, and despite several studies finding either no difference or even increased FC in ASD [18–20]. The inconsistencies of the results across studies could be driven by false positives, publication bias, small sample sizes, age effects, heterogeneity in the ASD population and co-occurring conditions such as intellectual disability, among other factors. These ambiguities highlight the need for a hypothesis-free evaluation of PS and FC in a large sample of ASD, focusing on replicability and generalizability.

Here, we evaluated resting state EEG PS and FC in ASD ($n=212$) and NT ($n=199$) children, adolescents and adults (all with $IQ>75$), using the baseline visit of the Longitudinal European Autism Project (LEAP) for a cross-sectional analysis [21, 22]. We focused on diagnostic effects and compared ASD and NT groups. In light of the conflicting literature, we performed a hypothesis-free evaluation of PS and FC without restriction on the frequencies, brain/scalp areas of interest, and directionality. We adopted a flexible analytical approach testing various models and evaluated the generalizability of our findings. To this end, we used cluster-based permutation statistics, which optimally account for the dimensionality of the data, to control for multiple testing across source locations and frequencies within specific models. Importantly, we used a validation dataset to test any findings from the main analysis and thereby account for possible false positives due to testing of multiple models.

Materials and methods

Study design and EEG acquisition

The resting state EEG data analyzed here were recorded as part of EU-AIMS LEAP. A complete description of the study design and clinical characterization of the participants can be found elsewhere [21, 22]. Briefly, participants with ASD were recruited based on an existing clinical diagnosis of ASD according to DSM-IV, DSM-IV-TR, DSM-5 or ICD-10 criteria and all participants were between 6 and 32 years. ASD symptomatology was assessed with various instruments including the Autism Diagnostic Observation Schedule-2 (ADOS-2) and the Autism Diagnostic Interview-Revised (ADI-R), but participants were not excluded based on ADOS-2 and ADI-R scores. In this work, we only include autistic

individuals with average to high intellectual capacities ($IQ > 75$) who successfully completed the resting state EEG recording (211 NT and 242 ASD).

Four minutes of resting state EEG were recorded per participant (2 min with eyes open, 2 min with eyes closed). To optimize participant compliance, resting state was acquired in 30 s blocks, alternating eyes open (fixating a physical hourglass) and eyes closed. Data were acquired at five sites: Central Institute of Mental Health (CIMH, Mannheim, Germany), King's College London (KCL, United Kingdom), University Nijmegen Medical Centre (RUNMC, Netherlands), University Campus BioMedico (UCBM, Rome, Italy) and University Medical Centre Utrecht (UMCU, Netherlands). The following EEG systems were employed: Brainvision (CIMH, KCL, RUNMC), Biosemi (UMCU) and Micromed (UCBM), with sampling frequencies of 5000 Hz (KCL, RUNMC), 2048 Hz (UMCU), 2000 Hz (CIMH) and 256–1000 Hz (UCBM). All sites used 10–20 layout caps, with 60–70 electrodes.

EEG data processing

Preprocessing

EEG signals were resampled to 1000 Hz and then band pass filtered to [1–32] Hz with a finite impulse response filter of order 2000 (using 2 s of padding at each edge of a resting state block). Higher frequencies (in the gamma range) were not included in the analysis to avoid substantial contamination with muscle activity [23]. Only data from 61 electrodes common to most contributing sites were retained for subsequent analyses. Preprocessing was performed manually and blinded to the participants diagnosis and clinical information, following these sequential steps: (a) Eliminate bad channels, (b) locate and discard sections with large transient artifacts resulting, e.g., from muscle bursts or movements, (c) perform independent component analysis with fastICA (<http://www.cis.hut.fi/projects/ica/fastica/>, [24]), (d) detect artefactual components (capturing: ocular, muscular, cardiac or other artifacts), (e) eliminate the contribution of artefactual components, (f) iterate points (b–e) if necessary, (g) interpolate the bad channels that were eliminated in (a), and (h) re-reference signals to the average across all channels (average reference).

Participants were excluded from subsequent analyses if they met any of the following criteria: (1) less than 15 clean 2.5 s epochs in the eyes-open or the eyes-closed condition (11 participants), (2) less than 51 usable channels or more than 3 neighboring channels eliminated (9 further participants), (3) number of good channels minus number of artefactual independent components smaller than 35 (threshold selected visually when inspecting the distribution of values, 6 further participants). Following

these criteria, 26 recordings (18 ASD and 8 NT) were discarded, resulting in a sample size of 224 ASD and 203 NT.

Summary resting state alpha measures

We inspected the alpha peak of each participant. Alpha is the most prominent rhythm in the resting EEG and could reveal if there was a shift in frequencies between the ASD and the NT groups (e.g., one group having alpha at higher frequencies than the other). Power spectra were computed for each channel and condition (eyes open and eyes closed) with fast Fourier transform and 2.5 s Hanning windows with 75% overlap. Alpha peaks in the [6, 13] Hz range were detected automatically by fitting a Gaussian over a power law background to the average eyes closed power spectrum over occipital channels O1, O2, Oz, PO4, PO3 and POz, following [25]. A single alpha peak frequency was derived per participant (and not separate ones for eyes open and eyes closed). Automatic fits were verified by visual inspection and refined for 11 out of 224 ASD and 10 out of 203 NT participants. Seven participants with no clear alpha peak were discarded from subsequent analyses, yielding a total of 218 ASD and 202 NT participants.

The following summary alpha measures were derived from the alpha peak: (1) alpha peak frequency f_p , (2) alpha power, defined as the absolute power in the range $[f_p - 2\text{Hz}, f_p + 2\text{Hz}]$ over occipital sensors (O1, O2, Oz, PO4, PO3, POz), (3) reactivity to eye opening, defined as $R = 1 - \frac{P_{EO}}{P_{EC}}$, where P_{EO} and P_{EC} are absolute power values defined previously for the eyes-open and the eyes-closed condition.

Source reconstruction

Head models with realistic geometry were built from individual's T1 weighted MRIs. Details on MRI acquisition can be found in [26]. T1-weighted MRIs were segmented with SPM12 [27] into gray matter, white matter, cerebrospinal fluid, bone, soft tissue and air. Then, these probabilistic images were smoothed (5 mm FWHM), thresholded and resliced to produce binary masks of $2\text{ mm} \times 2\text{ mm} \times 2\text{ mm}$ resolution for three tissue types: brain (including gray matter, white matter and cerebrospinal fluid), skull and scalp. These binary masks were transformed to hexahedral meshes with FieldTrip [28]. All three considered tissue types were assumed to have homogeneous and isotropic conductivity: 330 mS/m for the brain and scalp [29], and an age-dependent skull conductivity of $3.958 + 62.77 \cdot \exp(-0.2404 \cdot \text{age}[\text{years}])$ mS/m, in line with the BESA (BESA, Gräfelting, Germany) recommended conductivity ratios. Of note, the conductivity of cerebrospinal fluid is higher than that of gray or white matter [30], so setting the conductivity

of the brain compartment as a constant and isotropic value is a simplification, but the 3-tissue model has led to similar spatial accuracy than a model including a separate CSF tissue in a previous publication [31]. Segmentations were visually inspected, and for 9 participants head models could not be built (because of either no MRI or no clean segmentations). As a consequence, subsequent analyses included 212 ASD and 199 NT participants.

The forward model was derived with FieldTrip and SimBio [32]. 365 source locations of interest were defined in gray matter in MNI space, following a 3D cubic diamond grid with 1.5 cm spacing. Source positions were transformed from MNI to each subject's individual space with a nonlinear transformation obtained with SPM12. Electrode positions were determined by transforming standard MNI positions to subject's space with this same transformation and projecting to the scalp surface. Source time series were estimated with linearly constrained minimum variance beamformer, using a regularization of 5% of the average trace of the covariance matrix, a common filter for resting state eyes open and eyes closed and projecting the source time series into the direction of maximal power [33].

Power spectrum (PS)

Power spectra were computed for each sensor, source and condition: Time series (source or sensor) were convolved with Morlet wavelets of 0.6 octave frequency resolution ($f/\sigma_f=4.88$) and $5 \cdot \sigma_t$ window length, with 90% overlap between windows, for frequencies $f = 2^{1:0.15:5}$ Hz (frequencies from 2 to 32 Hz in increments of 0.15 in the exponent value). Since beamformer reconstructions suffer from power bias especially for deeper sources [34], source space PS values were normalized with the overall power over the [2 32] Hz range to produce relative PS values. Of note, all subsequent analyses were performed with source space data, except for a control analysis using absolute power at the sensor level.

Functional connectivity (FC)

The 365 sources (see above) were grouped into 50 regions of interests (ROIs) (25 symmetrical ROIs per hemisphere, obtained through k-means clustering of the source positions, leading to 4–13 sources per ROI). The representative time series for a given ROI was defined as the first principal component of all the source time series in this ROI. For each combination of ROIs and frequency, functional connectivity (FC) was quantified with orthogonalized power correlations (orthPowCorr) and weighted phase lag index (wPLI), which evaluate complementary phase and amplitude synchronization while discarding zero-lag synchronization which could be driven by volume conduction. OrthPowCorr and

wPLI were implemented following [35] and [36], respectively. In order to avoid introducing sample size-related bias in wPLI, resting state data were segmented into non-overlapping 2.5 s clean epochs, and wPLI was estimated across 15 epochs. These 15 epochs were selected randomly from all the clean epochs from a given subject and condition, this process was repeated 100 times, and values were averaged across the 100 repetitions. Control analyses with other FC metrics are performed using direct power correlations (PowCorr), coherence (COH), imaginary coherence (iCOH) and phase locking value (PLV), following [6, 35, 37]. More details on the FC metrics can be found in Additional file 1.

Participants

The statistical analyses reported in subsequent sections were performed using 212 ASD and 199 NT participants, after discarding 42 participants because of unsuccessful preprocessing, lack of clear alpha peak or no available head model (26, 7 and 9 participants, respectively, as detailed in previous sections). The groups of included and excluded autistic participants differed significantly, at the uncorrected group level, on Vineland (Adaptive Behaviors subscale scores) and ADOS-2 (Restricted and Repetitive Behaviours scores), with higher symptomatology in the excluded group (see Additional file 1 Table S1 for more details). This might be expected since participants with higher symptom expression are less likely to be able to comply with instructions, and more likely to move or generate artifacts during the EEG and MRI acquisition sessions. Table 1 summarizes the main demographics and clinical characteristics of the included participants. Age and sex did not differ between groups ($p=0.71$ and $p=0.24$, respectively). Similarly, the amount of clean data did not differ significantly ($p>0.15$) between groups for eyes open (ASD: mean 102 s, SD 13 s, range 55–120 s; NT: mean 104 s, SD 14 s, range 46–120 s) or eyes closed (ASD: mean 104 s, SD 13 s, range 60–125 s, NT: mean 106 s, SD 13 s, range 58–120 s) conditions.

Statistical analysis: data-driven exploration followed by validation in independent sample

We opted for a hypothesis-free statistical analysis rather than a targeted approach testing concrete hypotheses given that the ASD resting state literature is contradictory and a variety of effects across brain rhythms and brain regions have been reported. We assessed potential power spectra and FC alterations across frequencies and brain regions. Furthermore, we evaluated the generalizability of our outcomes by evaluating the impact of several analyses choices such as FC metric, statistical models, or ASD definition. In order to do so, while maintaining high statistical flexibility, we followed a train/validation approach. That is, we

Table 1 Overview of clinical and demographic characteristics of the participants included in the statistical analyses

	ASD	NT	Group differences
<i>n</i>	212	199	
Age (years)	16.6 ± 5.7 [6.7–30.3]	16.8 ± 6.0 [6.9–30.8]	$d = -0.04$ $p = 0.71$
Child/Adol/Adult	53/76/83	54/69/76	
IQ	104.0 ± 14.5 [75.6–148.0]	107.9 ± 13.1 [75.6–142.0]	$d = -0.28$ $p = 0.0045$
Sex (M/F)	153/59	132/67	$p = 0.24$
ADI social	15.3 ± 6.9 [0–29] ($n = 202$)		
ADI-R communication	12.5 ± 5.6 [0–26] ($n = 202$)		
ADI-R RRB	4.2 ± 2.8 [0–12] ($n = 202$)		
ADOS-2 Social Affect CSS	5.9 ± 2.6 [1–10] ($n = 209$)		
ADOS-2 RRB CSS	4.6 ± 2.6 [1–10] ($n = 209$)		
ADOS-2 Total CSS	5.1 ± 2.7 [1–10] ($n = 209$)		
VABS	74.4 ± 14.2 [20–121] ($n = 174$)	103.2 ± 11.7 [70–127] ($n = 48$)	$d = -2.21$ $p < 0.0001$
SRS-2	84.6 ± 31.2 [20–163] ($n = 193$)	25.0 ± 16.5 [1–94] ($n = 168$)	$d = 2.39$ $p < 0.0001$
Medication (%)	36.9% ($n = 198$)	5.6% ($n = 179$)	$p < 0.0001$

Child Children (age 6–11), *Adol* Adolescents (age 12–17), and adults are aged 18 years and above, IQ—full scale IQ, *M* male, *F* female, ADI social, ADI communication and ADI RRB refer to the Social, Communication and Restricted and Repetitive Behaviours total domain scores of the ADI-R (Autism Diagnostic Interview-Revised). ADOS Social Affect, ADOS RRB and ADOS Total refer to the Social Affect, Restricted and Repetitive Behaviours and Total calibrated severity scores in ADOS-2. VABS refers to the Vineland Adaptive Behavior Second Edition Adaptive Behavior Composite standard score. SRS-2 refers to the Social Responsiveness Scale-2 Total score (combined parent- and self-report). Medication refers to brain active medication (antidepressants, antimigraine, antipsychotics, anxiolytics, hypnotics, sedatives, psychostimulants, analgesics, etc.). Values from numerical variables are reported as mean ± standard deviation [min–max]. *P* values for the group effects are indicated (*t* test for continuous variables, Fisher's exact test for categorical variables) along with Cohen's *d*

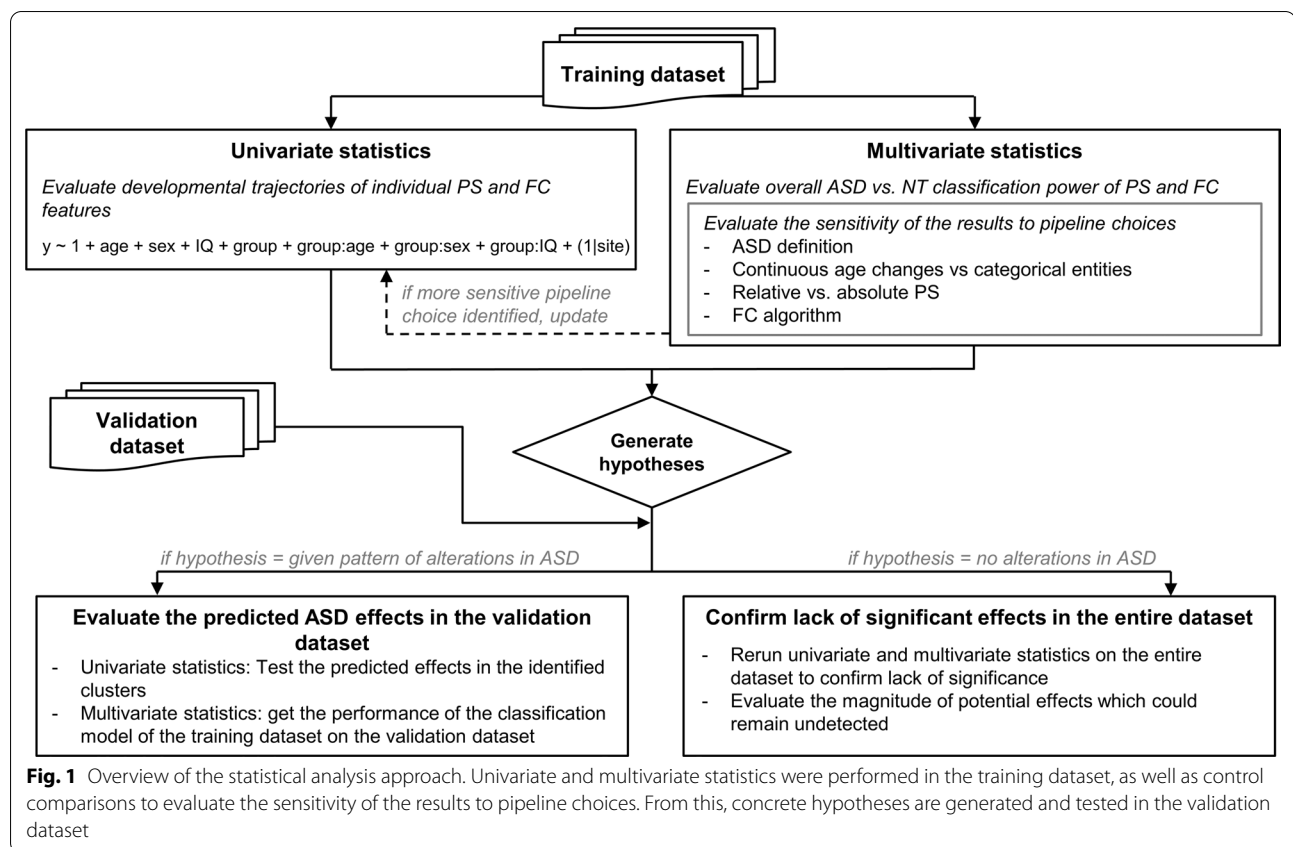
separated the dataset into training (70% of the participants: 147 ASD and 140 NT) and validation datasets (30% of the participants: 65 ASD and 59 NT). The 30%–70% split was performed using stratified randomization by site, age group (children, adolescents, adults) and diagnosis. The univariate and multivariate statistics described in the following sections were performed using the training dataset exclusively. Clear hypotheses were derived from the analyses in the training dataset, which were then tested in the validation dataset. To assess the consistency between results in the training and validation datasets, prediction intervals were calculated for the univariate analysis. They estimate the range of values that can be expected in a replication due to chance and were calculated following [38] for comparing effect sizes. An overview of the statistical approach is shown in Fig. 1. Clinical and demographic characteristics of the participants in the training and validation datasets can be found in Additional file 1: Tables S2 and S3.

Univariate statistics

Each summary alpha measure, PS and FC feature was submitted to the following linear mixed effects (LME) models:

$$\begin{aligned}
 y &\sim 1 + \text{age} + \text{sex} + \text{IQ} + (1|\text{site}), \text{homoscedastic residual errors} & (\text{model 1}) \\
 y &\sim 1 + \text{age} + \text{sex} + \text{IQ} + \text{group} + \text{group} : \text{age} + \text{group} : \text{sex} + \text{group} : \text{IQ} + (1|\text{site}), & (\text{model 2}) \\
 &\text{homoscedastic residual errors} \\
 y &\sim 1 + \text{age} + \text{sex} + \text{iq} + \text{group} + \text{group} : \text{age} + \text{group} : \text{sex} + \text{group} : \text{IQ} + (1|\text{site}), & (\text{model 3}) \\
 &\text{heteroscedastic residual errors}
 \end{aligned}$$

All models were fit with the nlme package in R version 3.4.0 [39], using maximum likelihood estimation. Models 1 and 2 assumed homoscedastic residual errors, while model 3 allowed for different residual variances in the ASD and NT groups. Model 3 is the full model shown in Fig. 1. Age and IQ were mean centered and variance normalized before entering the statistical models. The statistical significance of group differences in mean was determined through the log-likelihood ratio between models 2 and 1. Log-likelihood tests have been reported to be “anticonservative”: They may output *p* values that are lower than the nominal *p* values [40]. Therefore, significant group effects were confirmed by using *F*-tests on the individual parameters after fitting the models with a restricted maximum likelihood method [39]. The statistical significance of group differences in variance was determined through the log-likelihood ratio between models 3 and 2. The following transformations were applied before LME in order to convert the feature distributions to normality: $x \rightarrow \log(x)$ (absolute power), $x \rightarrow x^4$ (alpha reactivity), $x \rightarrow a \tanh(x)$ (orthPowCorr) and $x \rightarrow x^{0.11}$



(wPLI). The optimal transformations to normality were obtained by evaluating the Kolmogorov–Smirnov goodness-of-fit test for several families of transformations. For information on site and medication effects, refer to Additional file 1.

Cluster-based permutation tests were used to control for multiple comparisons for the PS and FC measures, following [41]. First, clusters of frequencies and electrodes/sources/links with significant effects ($p < 0.05$, uncorrected) were created. For PS, two sources/electrodes were considered neighbors if they were spatially adjacent. For FC, two links were considered neighbors if they had one common node and one spatially adjacent node. (Two ROIs are considered adjacent if they have at least one pair of neighboring sources.) Then, the cluster size was compared with the null-hypothesis distribution derived from the maximal cluster sizes obtained in randomized datasets (2000 randomizations were performed by randomizing group labels exclusively). P values were defined as the proportion of randomizations, which yielded a larger cluster size than the original dataset.

Multivariate statistics

To test whether a multivariate combination of PS and FC features, respectively, can discriminate ASD from NT, we

used machine learning techniques. Before subjecting the data to the multivariate analyses, the effects of age, sex, IQ and site were removed by building PS and FC datasets containing the residuals of the LME models $y \sim 1 + \text{age} + \text{sex} + \text{IQ} + (1|\text{site})$ trained on individual PS and FC features. The PS dataset consists in the space x frequency PS values for eyes-open and eyes-closed condition (19,710 features). The FC dataset contains FC strength across links, frequencies and conditions (66,150 features). Principal component analysis was applied to the PS and FC datasets (matrices of EEG features x subjects), and the principal components explaining at least 98% of the variance were used as input for the classification algorithms (160, 392 and 389 components for PS, OrthPowCorr and wPLI, respectively; each of these principal components is a linear combination of EEG features).

To date, a plethora of classification approaches has been introduced and proven useful [42]. The performance of the models depends greatly on the feature selection approach, classification algorithm and hyperparameter values. Here, we use three different classification approaches that have been successfully used in previous neuroimaging studies and are implemented with scikit-learn [43]: First, we use the L2-penalized support vector classifier (linSVC) which is one of the

most common approaches in neuroimaging [44, 45]. Second, we estimate an elastic net logistic regression, which combines L1 and L2 regularization and could perform better if only a small number of features was sufficient for the differentiation between two groups [45, 46]. Third, we combine a Boruta feature selection (based on random forests) with a radial basis kernel support vector classifier, which can detect nonlinear patterns differentiating between two groups [47]. Classifier hyperparameters were tuned using grid search (`sklearn.model_selection.GridSearchCV`) and nested tenfold cross-validation. The harmonic mean of sensitivity and specificity (also known as S1 score) was employed as the scoring metric, since it prevents algorithmic convergence into a trivial single class prediction in unbalanced datasets [48]. Further details on the classification models employed can be found in Additional file 1: Table S4. Repeated random splits [49] were used to evaluate the cross-validation performance of the classification models (15 random splits with 20% left-out data, using `sklearn.model_selection.StratifiedShuffleSplit`) within the training set. The significance of the classification performance of the classifiers was assessed by comparing the scoring metric in the original PS and FC datasets with the corresponding values

obtained when training the classifiers in datasets with randomized group labels (1000 randomizations).

Results

Univariate statistics

First, we studied properties of the EEG alpha peak, the most prominent feature of the awake human EEG. As expected from the literature, both the alpha peak frequency and absolute power significantly changed with age, with increasing peak frequency and decreasing power (Fig. 2, p values for age coefficient: alpha peak frequency $p=7.0\cdot10^{-11}$, absolute power eyes open $p=3.2\cdot10^{-17}$, absolute power eyes closed $p=1.9\cdot10^{-9}$). We next investigated whether the groups differed in mean or variance. (A higher variance in the ASD group could be indicative of increased variability or heterogeneity.) The mean reactivity to eye opening differed between the ASD and NT groups (log-likelihood test $p=0.042$): There was a significant interaction between group and age (F -test, $p=0.048$): The age-related increases in reactivity were stronger in the NT than in the ASD cohort. We found no significant differences between ASD and NT for alpha peak frequency or absolute power in the training sample and no difference between variances for any measure ($p>0.12$, Table 2).

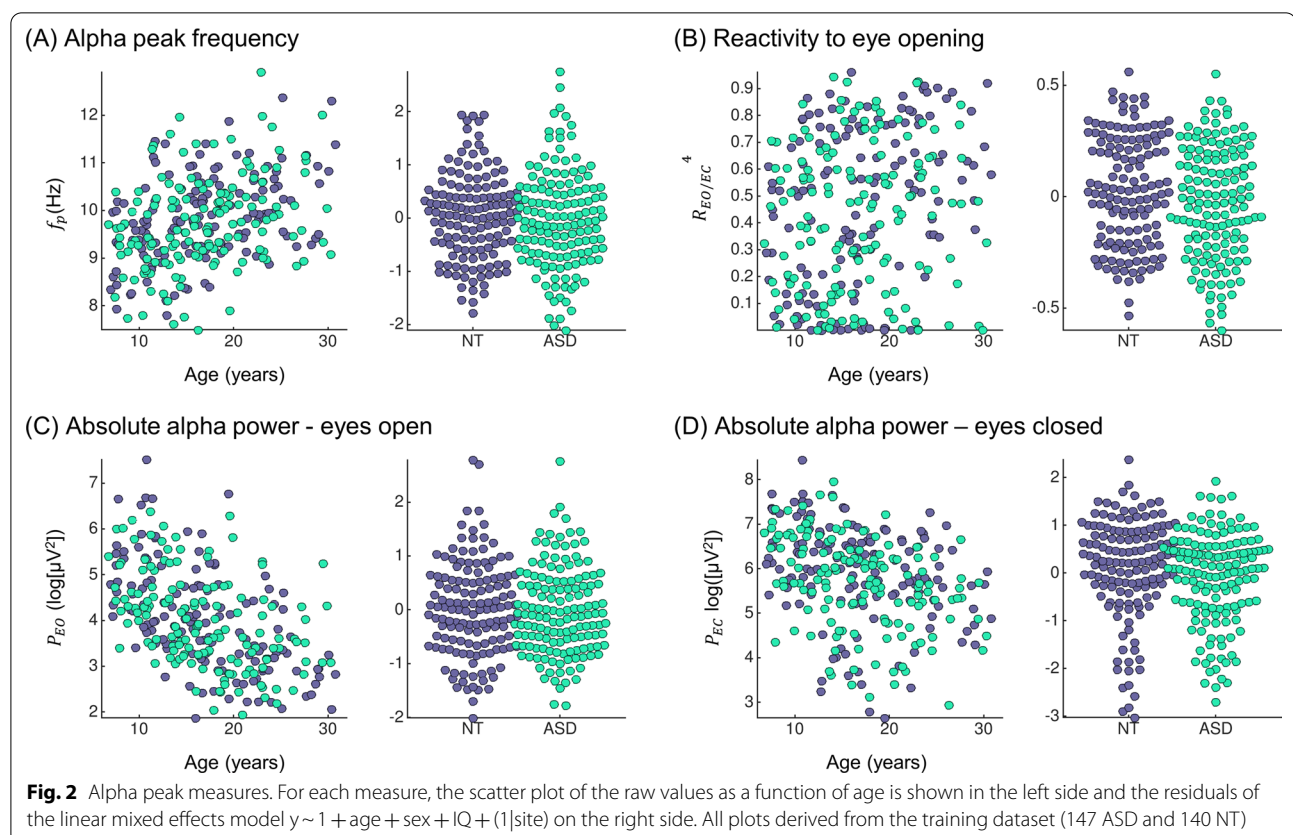


Table 2 *P* values from the univariate statistics (training dataset, 147 ASD and 140 NT)

	Differences in mean		Differences in variance	
Alpha peak frequency	0.77 ($d = -0.11$)		0.12	
Reactivity to eye opening	0.042 ($d = -0.18$)		0.76	
	Eyes open	Eyes closed	Eyes open	Eyes closed
Absolute alpha power	0.43 ($d = -0.05$)	0.39 ($d = -0.20$)	0.37	0.28
Power spectrum	0.72 ($d = -0.05$)	0.91 ($d = 0.27$)	0.53	0.92
wPLI	0.90 ($d = -0.24$)	0.98 ($d = -0.05$)	0.89	0.23
OrthPowCorr	0.59 ($d = -0.15$)	0.91 ($d = 0.12$)	0.39	0.85

P values were obtained after comparing the log-likelihoods of the three linear mixed effects models (see Materials and Methods). For power spectrum, wPLI and OrthPowCorr, *p* values were derived from cluster-based permutation tests. Cohen's *d* values are given for reference after the *p* values, but note that they do not directly reflect statistical significance, since they were computed with the raw EEG parameters and do not correct for any covariates. wPLI: Weighted phase lag index. OrthPowCorr: Orthogonalized power correlations. *P* values under 0.05 are highlighted in bold

Next, we investigated source space spectral power and functional connectivity. As expected from the literature, both PS and FC were strongly modulated by age. Cluster-based permutations tests showed two clusters of PS modulations with age ($p < 0.001$, log-likelihood tests of models with and without age coefficients): with PS decreasing with age for lower frequencies (< 7.7 Hz) and increasing for higher frequencies (> 10.6 Hz). Note that opposite trends in both frequency ranges are expected given the use of relative power. Comparing ASD to NT, we did not find any significant group effects for PS or FC, neither for mean nor for variance ($p > 0.05$, correcting for multiple comparisons with cluster-based permutation tests within PS and FC, respectively; Table 2).

Multivariate statistics

We next investigated whether a multivariate combination of PS and FC features across space and frequency could separate ASD from NT using three machine learning approaches: linear SVC, elastic net logistic regression and radial basis function SVC with a nested Boruta feature selection (see Methods). Classification performance was overall poor (accuracy 47–57%, sensitivity 50–54%, and specificity 44–61%). For PS and wPLI, the classification performance with the elastic net classifier was greater than expected by chance ($p = 0.025$ and $p = 0.009$, respectively, Table 3).

Generalizability: age, ASD definition, alternative PS and FC measures

Our results above depend on specific analysis choices including accounting for age as a covariate, criteria for inclusion in the ASD group and choice of specific PS and FC metrics. We next tested whether our results were robust to these specific choices. First, to account for possible nonlinear age dependencies, we built separate ASD vs. NT classification models for children (6–11 years),

adolescents (12–17 years) and adults (18–32 years). Such models could uncover potential age-group specific ASD patterns (e.g., alterations only in adults, or only in children and adults but not adolescents) without committing to a pre-specified age-dependency model. Secondly, we used an alternate and “narrower” ASD definition and restricted the ASD sample to individuals who in addition to the ASD clinical diagnosis also met the ASD threshold on the ADOS-2 and on the ADI-R, following [50]. 51.8% of the ASD participants met this additional criterion ($n = 77$ ASD participants in the training dataset, $n = 110$ ASD participants overall, see Additional file 1: Table S5 for a full description of their clinical and demographic characteristics). Thirdly, the effect of EEG processing pipeline choices was assessed by evaluating absolute rather than relative power and alternate FC algorithms with different underlying assumptions on the nature of the coupling between regions' activities (PowCorr, COH, iCOH and PLV, as described in Materials and Methods). The results are listed in Table 3. Of note, given the amplitude bias in beamforming source reconstructions, absolute power was estimated in sensor space. Classification performance was in general poor and in line with the main analysis described in the previous section, and only significantly better than expected by chance for the linear SVC and the elastic net model with wPLI in children ($p = 0.02$ and $p = 0.013$, respectively).

Testing the models in the validation dataset

Data of 30% of the participants (65 ASD and 59 NT) were hold out from the previous analyses, in order to enable validation of the effects identified in the training dataset (significant group effects for reactivity to eye opening and classification performance for PS and wPLI):

- Reactivity to eye opening was not significantly modulated by group in mean or variance in the valida-

Table 3 ASD vs NT cross-validation classification performance of PS and FC features (training dataset)

Age groups	Diagnosis	Measure	Linear SVC				Elastic net				Boruta + rbf SVC			
			acc	sens	spec	p-val	acc	sens	spec	p-val	acc	sens	spec	p-val
All	ASD	PS	0.52	0.53	0.51	0.24	0.56	0.52	0.59	0.025	0.54	0.54	0.54	0.08
All	ASD	OrthPowCorr	0.48	0.50	0.45	0.81	0.50	0.51	0.49	0.45	0.53	0.52	0.53	0.18
All	ASD	wPLI	0.47	0.50	0.44	0.79	0.57	0.53	0.61	0.009	0.53	0.50	0.55	0.19
<i>Build separate models for adults, adolescents and children</i>														
Adults	ASD	PS	0.50	0.48	0.51	0.50	0.48	0.45	0.52	0.63	0.49	0.50	0.48	0.49
Adolescents	ASD	PS	0.49	0.47	0.51	0.60	0.50	0.50	0.51	0.50	0.48	0.46	0.50	0.56
Children	ASD	PS	0.53	0.51	0.55	0.29	0.47	0.51	0.44	0.68	0.43	0.45	0.42	0.84
Adults	ASD	OrthPowCorr	0.56	0.63	0.49	0.09	0.50	0.48	0.53	0.44	0.47	0.50	0.45	0.76
Adolescents	ASD	OrthPowCorr	0.45	0.51	0.39	0.78	0.50	0.49	0.52	0.40	0.53	0.60	0.46	0.29
Children	ASD	OrthPowCorr	0.60	0.48	0.71	0.07	0.49	0.47	0.51	0.66	0.46	0.44	0.47	0.77
Adults	ASD	wPLI	0.54	0.63	0.45	0.30	0.50	0.45	0.55	0.52	0.52	0.53	0.52	0.31
Adolescents	ASD	wPLI	0.48	0.44	0.53	0.53	0.44	0.43	0.45	0.87	0.43	0.44	0.42	0.91
Children	ASD	wPLI	0.64	0.54	0.73	0.02	0.60	0.62	0.59	0.013	0.47	0.36	0.56	0.73
<i>Use a narrower ASD definition</i>														
All	ASDn	PS	0.53	0.39	0.61	0.45	0.55	0.55	0.56	0.17	0.56	0.48	0.61	0.15
All	ASDn	OrthPowCorr	0.59	0.18	0.82	0.48	0.50	0.52	0.49	0.42	0.53	0.37	0.62	0.79
All	ASDn	wPLI	0.55	0.22	0.73	0.34	0.48	0.53	0.46	0.44	0.55	0.42	0.62	0.26
<i>Evaluate other variations of EEG power spectral and functional connectivity algorithms</i>														
All	ASD	abs. PS	0.51	0.51	0.51	0.36	0.53	0.54	0.51	0.14	0.51	0.51	0.52	0.36
All	ASD	PowCorr	0.47	0.48	0.46	0.81	0.46	0.45	0.47	0.99	0.49	0.49	0.48	0.68
All	ASD	PLV	0.47	0.49	0.45	0.82	0.51	0.50	0.53	0.63	0.52	0.52	0.52	0.28
All	ASD	iCOH	0.48	0.53	0.42	0.81	0.46	0.45	0.48	0.87	0.49	0.51	0.47	0.65
All	ASD	COH	0.46	0.47	0.44	0.91	0.47	0.45	0.49	0.88	0.48	0.49	0.47	0.74

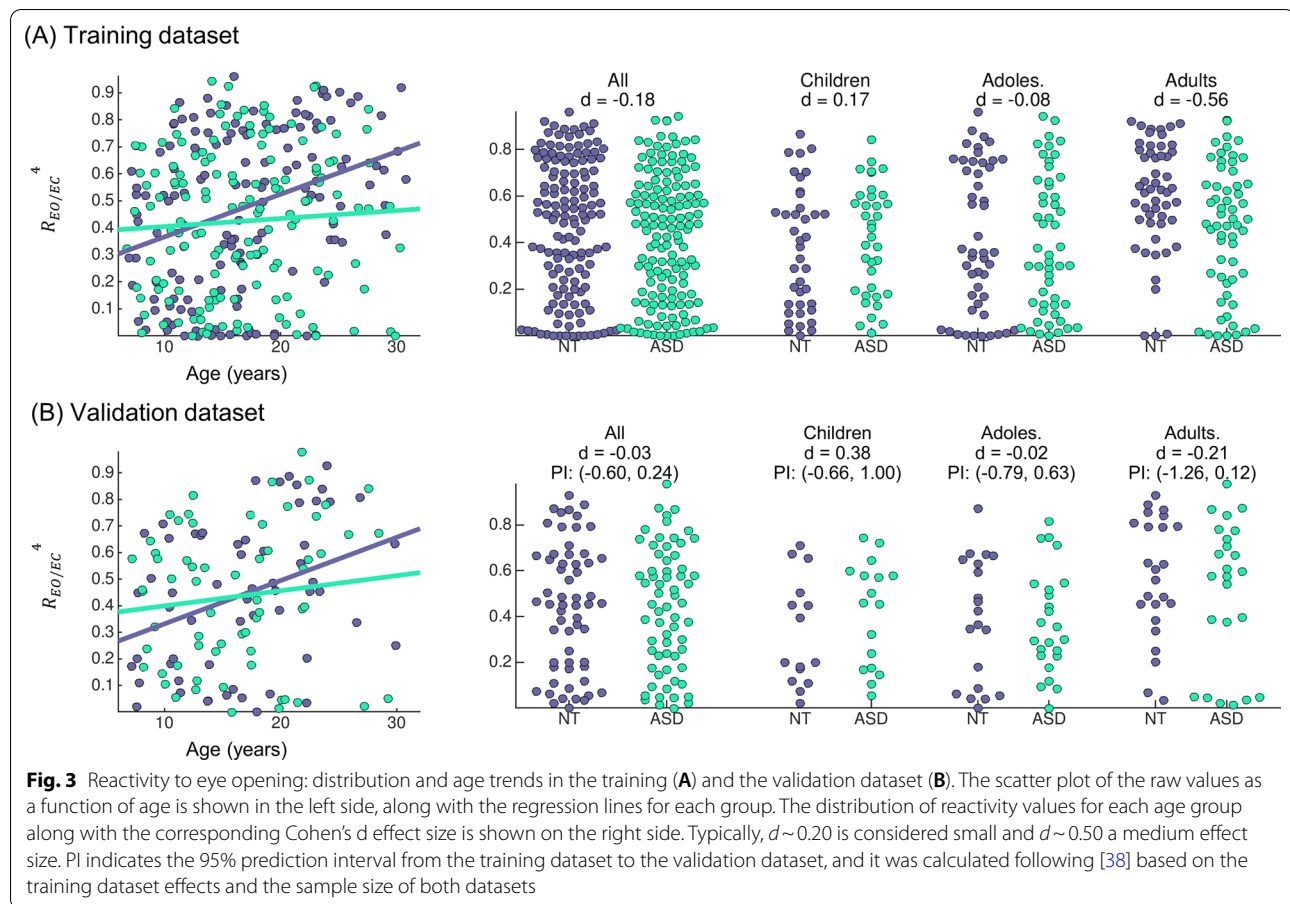
Accuracy (acc), sensitivity (sens), specificity (spec) and the p value derived from randomization tests are indicated. Classifiers with $p < 0.05$ are highlighted in bold. abs. PS refers to absolute power spectrum and was obtained in sensor space

tion dataset ($p > 0.5$). Some trends similar to those present in the training dataset can be found in the validation dataset: stronger increase with age in the NT than in the ASD group, and reduced values in adults in ASD compared to NT, see Fig. 3. However, these effects were weak and not significant. Although group effects were not significant, the effect sizes of the case–control alterations across age groups in the validation dataset fell within the 95% prediction intervals of the effects seen in the training dataset, indicating that random variability within the ASD and NT groups alone could account for the deviation of values observed between training and validation dataset. See Fig. 3 for a full overview of effect sizes and prediction intervals across age groups.

- Classification ASD vs NT. The four classification models that produced a significant cross-validation classification performance in the training dataset ($p < 0.05$) were tested in the validation dataset. The results are shown in Table 4. Classification performance was overall poor (accuracy 38–57%) and only above 50% for the elastic net model on PS ($p = 0.073$

compared to randomized versions of the validation dataset). These performance values were in line with those obtained with cross-validation in the training dataset, as shown in Fig. 4.

In summary, all the ASD vs NT alterations found in the training dataset were not significant in the validation dataset (ASD group effects $p > 0.05$), despite showing similar trends for reactivity to eye opening and PS elastic net model. This could be due to sampling error and to limited statistical power for detecting weak effects in the validation dataset. This is illustrated by the following power considerations. The statistical power to detect an effect size (standardized mean difference) of 0.5 in the validation dataset is 72%, but if this effect is for example restricted to adults only (which could be the case for reactivity to eye opening training dataset), the statistical power is only 18%. This means that there is a high chance of not finding significant effects in the validation dataset even if the true ASD phenotype was close to that found in the training dataset and there was a weak interaction

**Table 4** Classification performance of the multivariate models tested in the validation dataset

Age groups	Measure	Classifier	acc	sens	spec	S1	p -val
All	PS	Elastic net	0.57	0.55	0.59	0.57	0.073
All	wPLI	Elastic net	0.48	0.46	0.51	0.48	0.68
Children	wPLI	Elastic net	0.38	0.41	0.33	0.37	0.96
Children	wPLI	Linear SVC	0.38	0.41	0.33	0.37	0.96

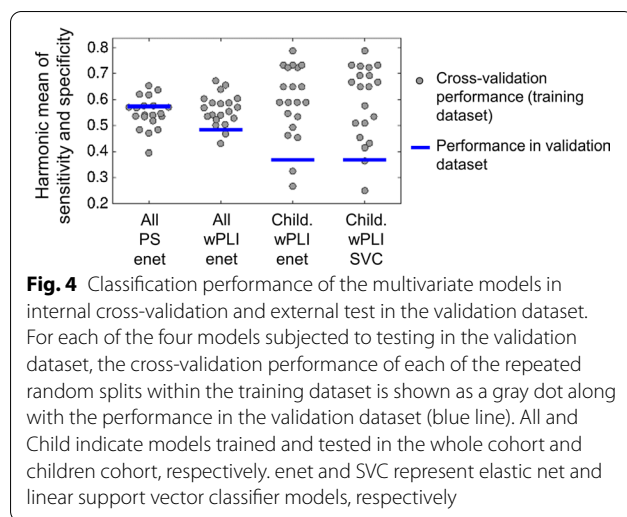
Accuracy (acc), sensitivity (sens), specificity (spec), S1 and the p value comparing the classification performance obtained in the original dataset with that of replicate datasets with randomized group labels is indicated for each model

between age and group. More details can be found in Additional file 1.

Discussion

We investigated differences in resting state EEG parameters between autistic and neurotypical individuals with average to high intellectual abilities from childhood to adulthood in a large and well-controlled cohort ($n = 212$ ASD and $n = 199$ NT). We analyzed various EEG metrics (alpha peak properties, PS, FC) that have been suggested to be altered in ASD. We examined whether the NT and ASD groups differed in either mean or

variance across PS and FC features using univariate testing along with cluster-based permutation tests. We then used machine learning to assess whether combining EEG features could unveil complex patterns separating ASD and NT participants. To test the generalizability of the results, alternative models using a stricter ASD definition and additional PS and FC endpoints were tested, as well as models trained in children, adolescents or adults-only. These analyses were embedded within a train-test approach to enable the testing of various models and underlying hypotheses while minimizing the likelihood of finding false positive results. In the training set,



we found significant differences between ASD and NT for three EEG metrics: (1) interaction between age and diagnosis for the reactivity to eye opening with stronger age-related increases in the NT than the ASD cohort (2) significant but rather weak classification performance for PS and wPLI across age groups and for wPLI in children (accuracy of 0.56–0.64, sensitivity 0.52–0.62, specificity 0.59–0.73). The effects in the validation dataset were non-significant, but they were in line with those found in the training dataset (overlapping with the training dataset's prediction interval or with internal cross-validation performance). This could be explained either by no consistent effects or by consistent albeit weak effects across both datasets.

Age-dependent maturation of brain rhythms

In line with previous studies of NT developmental trajectories, we observed the expected developmental changes of EEG features, such as age-related increases in alpha peak frequency, relative upper alpha/beta power and average FC [51–54]. This can be seen as a plausibility check for this dataset.

Our results in the context of the literature

Directly comparing our results with previous publications is complicated by heterogeneity in the methods (e.g., specific EEG parameter extracted, FC metric, regions of interest to estimate pairwise connectivity) and the ASD subpopulation (e.g., age range, IQ, sex). A careful comparison with prior work is nonetheless critical to inform future work with EEG in ASD. Of particular relevance to this effort is O'Reilly et al.'s prior systematic analysis of EEG/MEG FC literature [17]. They evaluated the support for two popular hypotheses in the ASD field—long-range hypoconnectivity and local

hyperconnectivity—and concluded that there was relatively strong support for long-range hypoconnectivity in ASD. However, heterogeneity in methods precluded a quantitative meta-analytic confirmation of this phenomenon or of which EEG parameter would best quantify it. Additionally, publications from the largest reviewed dataset [55, 56] enrolling 430 ASD and 554 NT found a mixture of long-range hypo- and hyperconnectivity, suggesting that the long-range hyperconnectivity hypothesis may not fully reflect the complexity of ASD. The authors found an impressive 86% ASD vs. NT classification accuracy, but we cannot test whether their results replicate in the LEAP dataset because their findings are based on a multivariate combination of thousands of features, and the exact combination of features and model weights is not available for download. Although the original study excluded high functioning autism and Asperger [56], the authors found that their original multivariate model also classified NT vs. Asperger with high accuracy [55], so the IQ range of the cohorts do not seem to be causing the discrepancy between their results and ours.

FC in ASD has also been extensively studied in fMRI. Some reviews indicate a consistent pattern of reduced fMRI cortico-cortical connectivity in ASD in adolescents and adults, with an associated and perhaps compensatory increase in short range connectivity [57–59]. In fact, fMRI FC alterations have also been found in the LEAP sample: with both hyperconnectivity in prefrontal and parietal cortices and hypoconnectivity in sensory-motor regions in ASD compared to NT [26]. This pattern of alterations was reproduced in two additional datasets, thereby confirming the robustness of the effects. While both fMRI- and EEG-derived FCs measure aspects of long-distance communication in the brain, the resulting FC values are different, as shown in [60]. Both modalities measure a different type of brain activity (synchronized neuronal activity for EEG, blood oxygenation for fMRI) and have distinct spatial and temporal resolution [61]. Future multimodal analyses comparing directly EEG- and fMRI-derived FC at the single subject level in ASD and NT would be best suited to understand whether the fMRI-derived ASD patterns have an EEG correlate.

Regarding PS, Edgar et al. published the largest study to date [62], with 183 ASD and 121 NT, and provided a testable hypothesis: an interaction between group and age in alpha peak frequency, with strong age-related increases in the NT group and no significant age effects in the ASD group. Within the LEAP dataset, we found age-related increases for both groups. Both datasets have a similar design (cross-sectional, similar age range, no lower IQ participants), so any difference in results is more likely to reflect other factors, such as differences in recruitment, and other more nonspecific effects (e.g., site effects

or sampling variability). However, LEAP results for the ASD group are not far from the prediction interval of Edgar et al.: They found $r=0.10$ in the ASD group, which according to [38] results in a prediction interval for LEAP of $[-0.10, 0.30]$ and that is close to the value we recovered ($r=0.33$). For the NT group, our results converge with Edgar and colleagues: They found $r=0.57$, which leads to a prediction interval $[0.41, 0.72]$ which in turn comprises the value obtained in LEAP ($r=0.44$).

Lack of a significant effect is not demonstrating no effect

It is important to highlight that a lack of significant effects is different from demonstrating that there are no group differences. Although we had access to a large cohort and would have consequently greater sensitivity to detect core ASD patterns than most previous studies, it is possible and indeed even plausible that there are differences between ASD and NT with smaller effect sizes that we may not have detected. That said, our work suggests that possible differences in resting state EEG features between ASD ($IQ > 75$) and NT have relatively low effects sizes, which may limit their utility.

We used statistical power simulations to illustrate and quantify the impact of sample size. Accordingly, our statistical power to detect a true alteration of effect size of 0.3 would be 62% in the training dataset, which means that there is a 38% chance of having missed such an effect. In the training dataset, we found a significant interaction between age and group in the reactivity to eye opening, with stronger age-related increases in NT than ASD and strongest different between both groups for the adult cohort ($ES = -0.57$). The ES in the training was -0.21 , which was in the 95% prediction interval from the training dataset, and there is therefore no evidence for discrepancy between both effects. In fact, our statistical power to detect ASD alterations of effect size 0.5 in adults only is 18%, indicating that the validation dataset is not well suited for testing such small age-group specific effects and the need for a bigger cohort to fully assess the reproducibility of these findings.

For multivariate statistics, we found weak classification performances in the training dataset (cross-validation accuracies 0.56–0.64), and in the validation dataset the PS classifier had an accuracy of 0.57 along with a trend for statistical significance ($p=0.073$). Although this classification pattern may reach significance in a bigger validation dataset, the performance in the training and validation dataset suggests that this is a rather weak classifier which may not have very useful clinical applications. Additionally, machine learning techniques often require a large sample size to achieve good predictive performance [63, 64]. A minimum of 10–20 observations (our in our case, subjects) per variable has

been suggested for reliable performance of machine learning methods [65, 66]. Our EEG PS and FC matrices have a high dimensionality, but these variables are correlated and most of their variance is captured in a much smaller number of components (160–389 for PS and FC). Accordingly, future studies with at least 1500 individuals could be therefore better suited to boost the performance of the classifiers. Additionally, although we chose three different and popular state of the art machine learning approaches, it is conceivable that other approaches would be more suited to the problem and to a potential true ASD pattern of alterations. We therefore cannot exclude that with more data and/or other algorithms a better ASD vs. NT separation can be achieved.

Heterogeneity and possible subgroups in ASD

The heterogeneity of ASD could underlie the lack of significant ASD vs NT differences. ASD has diverse clinical presentations and is in turn thought to be driven by diverse biological substrates [2, 67, 68]. In fact, ASD is common in genetic neurodevelopmental disorders that are characterized by specific and different, sometimes even “opposite” neurobiological and circuitry alterations. It may well be that idiopathic ASD could be split into subgroups of homogeneous neurobiology that substantially differ [3, 68] and possibly even deviate from NT in opposite directions. This could mean for EEG features that the subgroups would change in various directions and the mean might not differ from NT unless appropriate subgrouping is performed. If this were true, it may manifest as increased variance in the ASD group compared to the NT group. We investigated this possibility in the univariate analysis, but could not find any support for the idea that heterogeneous subgroups may drive differential variance in the ASD population as a whole, as compared to NT. Of note, we did not perform clustering in the ASD EEG PS and FC or attempt to find ASD subgroups, but rather focused on the variance of PS and FC measures in ASD compared to NT. Previous studies have used unsupervised statistical learning to identify clusters of ASD subjects based on clinical, behavioral or biological measures [69–71]. Additionally, some studies suggest that differences in brain structure and function in people with ASD are idiosyncratic [72–75]: They are peculiar to an individual person with ASD rather than following a group trend. In this view, each ASD individual could deviate from NT in a different set of features, and no substantial increase in the ASD group variance would be expected for individual PS or FC measures.

Other measures of brain activity and event-related potentials may provide more information on ASD pathophysiology

Paradigms and brain activity measurements other than resting state EEG may be more sensitive to capture ASD-specific brain circuitry alterations. Indeed, significant case–control effects have been found in previous analyses of resting state fMRI and task EEG in the baseline LEAP recordings. First, as mentioned earlier in the discussion, reproducible fMRI FC alterations have been found in the LEAP cohort [26]. Second, [76] showed an increase in the latency of the N170 component of the event-related potential to faces in ASD compared to NT in the LEAP cohort. The modulation of brain activity during tasks that challenge functions that are often altered in ASD may shed more light onto the ASD-specific circuitry than resting state activity. Interestingly, here we found trends for an effect in the reactivity to eye opening, which is a very basic sensory response measure. Other more elaborated EEG paradigms tapping into elements of sensory or social processing linked to the ASD symptomatology could show stronger effects [77–79].

Limitations

We cannot draw a firm conclusion on whether the effects on reactivity to eye opening and PS found in the training dataset are reproducible. These effects were weak and the validation dataset is underpowered to confirm them. We have addressed this by estimating prediction intervals and statistical power, as detailed in Results section. Additionally, this is a cross-sectional study and longitudinal data would enable a better estimation of the developmental trajectories of ASD and NT subjects and would lead to more power to detect subtle differences. Finally, here we have exclusively focused on case–control comparisons, but it is possible that other analyses assessing clustering or dimensional correlations with symptom severity could reveal patterns of PS or FC linked to ASD-related symptomatology. Moreover, in this study, we only investigated individuals with an IQ > 75. We opted for this approach because although the LEAP sample includes some individuals with an IQ below 75, they are only included in the adolescent and adult groups in a subset of sites, and we did not want to introduce confounding relations between variables. However, this means that our results may not generalize to people with ASD and intellectual disability or to syndromic forms of ASD. In fact, rare genetic neurodevelopmental disorders characterized by intellectual disability and a symptomatic overlap with ASD such as Fragile X, Angelman and Dup15q syndromes frequently have characteristic resting state EEG features [80–82].

Conclusions

We found no differences between ASD and NT in resting state EEG that reproduced significantly in the validation dataset, despite trends for reactivity to eye opening and PS. Importantly, alpha peak parameters, PS and FC showed strong and expected age-related maturation from childhood to adulthood in ASD and NT cohorts, demonstrating good data quality and validity of the analytical approaches. In sum, this could indicate, that, across brain rhythms, local and long-range synchronization in ASD (IQ > 75) may overlap largely with the NT distribution. Additionally, no evidence for increased heterogeneity in ASD was found, since the modeled variance in both groups did not differ significantly. Future work could focus on establishing the within-subject developmental trajectory in longitudinal studies, directly targeting the ASD heterogeneity with clustering techniques or evaluating further EEG metrics (e.g., complexity) to further test for specific signatures in the EEG of individuals with ASD.

Abbreviations

ADI-R: Autism Diagnostic Interview-Revised; ADOS-2: Autism Diagnostic Observation Schedule, 2nd edition; ASD: Autism spectrum disorder; COH: Coherence; EEG: Electroencephalography; FC: Functional connectivity; iCOH: Imaginary coherence; IQ: Intelligence quotient; LME: Linear mixed effects; MRI: Magnetic resonance imaging; NT: Neurotypical; orthPowCorr: Orthogonalized power correlations; PLV: Phase locking value; PowCorr: Direct power correlations; PS: Power spectrum; ROI: Region of interest wPLI: Weighted phase lag index.

Supplementary Information

The online version contains supplementary material available at <https://doi.org/10.1186/s13229-022-00500-x>.

Additional file 1. Supplementary Material. Supplementary tables and figures.

Acknowledgements

We thank all participants and their families for participating in this study. We also gratefully acknowledge the contributions of all members of the EU-AIMS LEAP group.

The EU-AIMS LEAP group authorship: Jumana Ahmad, Sara Ambrosino, Bonnie Auyeung, Tobias Banaschewski, Simon Baron-Cohen, Sarah Baumeister, Christian F. Beckmann, Sven Bölte, Thomas Bourgeron, Carsten Bours, Michael Brammer, Daniel Brandeis, Claudia Brogna, Yvette de Bruijn, Jan K. Buitelaar, Bhismadev Chakrabarti, Tony Charman, Ineke Cornelissen, Daisy Crawley, Flavio Dell'Acqua, Guillaume Dumas, Sarah Durston, Christine Ecker, Jessica Faulkner, Vincent Frouin, Pilar Garcés, David Goyard, Lindsay Ham, Hannah Hayward, Joerg Hipp, Rosemary Holt, Mark H. Johnson, Emily J.H. Jones, Prantik Kundu, Meng-Chuan Lai, Xavier Liogier D'ardhuy, Michael V. Lombardo, Eva Loth, David J. Lythgoe, René Mandl, Andre Marquand, Luke Mason, Maarten Mennes, Andreas Meyer-Lindenberg, Carolin Moessnang, Nico Mueller, Declan G.M. Murphy, Bethany Oakley, Laurence O'Dwyer, Marianne Oldehinkel, Bob Oranje, Gahan Pandina, Antonio M. Persico, Barbara Ruggeri, Amber Ruigrok, Jessica Sabet, Roberto Sacco, Antonia San José Cáceres, Emily Simonoff, Will Spooren, Julian Tillmann, Roberto Toro, Heike Tost, Jack Waldman, Steve C.R. Williams, Caroline Wooldridge, and Marcel P. Zwiers

Author contributions

SB, LM, EJH, Tba, SBC, SB, JKB, SD, BO, AMP, CFB, TB, FDA, CE, CM, TC, TBo, JT, DGMM, MJ, EL and DB contributed to designing the EU-AIMS study and

developing data acquisition protocols, data acquisition and study setup. SB, CHC, SH, JD, DB, LM and JFH designed the analysis pipeline. PG and JH prepared the data analysis pipeline and performed the analyses and result visualization. PG, SB, LM, CHC, SH, JD, EJHJ, DB and JFH made substantial contributions to the result discussion and interpretation. PG and JFH wrote the first draft. All co-authors have revised the manuscript and provided important intellectual content.

Funding

This work was supported by EU-AIMS (European Autism Interventions), which receives support from the Innovative Medicines Initiative Joint Undertaking under grant agreement no. 115300, the resources of which are composed of financial contributions from the European Union's Seventh Framework Programme (grant FP7/2007–2013), from the European Federation of Pharmaceutical Industries and Associations companies' in-kind contributions and from Autism Speaks. AIMS-2-TRIALS is funded by the Innovative Medicines Initiative 2 Joint Undertaking (IMI 2 JU) under grant agreement no. 777394. This Joint Undertaking receives support from the European Union's Horizon 2020 research and innovation program, EFPIA, Autism Speaks, Autistica, and SFARI. PG was supported by the Roche Postdoctoral Fellowship (RPF) program.

Availability of data and materials

Data collected in EU-AIMS LEAP are stored and curated at the central EU-AIMS database at the Pasteur Institute in Paris. The database is open to members of the wider scientific community upon request and submission of a paper and data analytic proposal.

Declarations

Ethics approval and consent to participate

The study was approved by the local ethical committees of the participating centers, and written informed consent was obtained from all participants or their legal guardians (for participants < 18 years).

Consent for publication

Consent for publication was obtained from all participants prior to the study.

Competing interests

JD is former, and PG, CHC, SH and JFH are current full-time employees of F. Hoffmann–La Roche Ltd. TBA served in an advisory or consultancy role for ADHS digital, Infectopharm, Lundbeck, Medice, Neurim Pharmaceuticals, Oberberg GmbH, Roche and Takeda. He received conference support or speaker's fee by Medice and Takeda. He received royalties from Hogrefe, Kohlhammer, CIP Medien, Oxford University Press. SB has acted as an author, consultant or lecturer for Medice, Roche, Hogrefe, Kohlhammer and UTB. JKB was a consultant to/member of advisory board of/and/or speaker for Janssen-Cilag BV, Eli Lilly, Takeda (Shire), Medice, Roche and Servier. CFB is director and shareholder in SBGneuro. DGMM has been a consultant to and advisory board member for Roche and Servier; he is not an employee of nor stock shareholder in any of these companies. JT is a consultant for F. Hoffmann–La Roche Ltd. TC has served as a paid consultant to F. Hoffmann–La Roche Ltd. and Servier and has received royalties from Sage Publications and Guilford Publications.

Author details

¹Roche Pharma Research and Early Development, Neuroscience and Rare Diseases, Roche Innovation Center Basel, Basel, Switzerland. ²Department of Child and Adolescent Psychiatry and Psychotherapy, Central Institute of Mental Health, Medical Faculty Mannheim, Heidelberg University, Mannheim, Germany. ³Department of Psychological Sciences, Centre for Brain and Cognitive Development, Birkbeck, University of London, London, UK. ⁴Institute of Neuroscience and Medicine, Brain and Behaviour (INM-7), Research Centre Jülich, Jülich, Germany. ⁵Medical Faculty, Institute of Systems Neuroscience, Heinrich Heine University Düsseldorf, Düsseldorf, Germany. ⁶Department of Psychiatry, Autism Research Centre, University of Cambridge, Cambridge, UK. ⁷Department of Women's and Children's Health, Center of Neurodevelopmental Disorders (KIND), Centre for Psychiatry Research, Karolinska Institutet and Child and Adolescent Psychiatry, Stockholm Health Care Services, Region Stockholm, Stockholm, Sweden. ⁸Curtin Autism Research Group, Curtin School of Allied Health, Curtin University, Perth, WA, Australia. ⁹Department

of Cognitive Neuroscience, Donders Institute for Brain, Cognition and Behaviour, Radboudumc, Nijmegen, The Netherlands. ¹⁰Brain Center Rudolf Magnus, University Medical Center Utrecht, Utrecht, The Netherlands. ¹¹Interdepartmental Program "Autism 0-90", "G. Martino" University Hospital, University of Messina, Messina, Italy. ¹²Human Genetics and Cognitive Functions, Institut Pasteur, UMR3571 CNRS, Université de Paris, Paris, France. ¹³Institute of Psychiatry, Psychology and Neuroscience, King's College, London, UK. ¹⁴Department of Child and Adolescent Psychiatry, Psychosomatics and Psychotherapy, University Hospital, Goethe University, Frankfurt am Main, Germany. ¹⁵Department of Child and Adolescent Psychiatry and Psychotherapy, Psychiatric Hospital, University of Zurich, Zurich, Switzerland. ¹⁶Neuroscience Center Zurich, University and ETH Zurich, Zurich, Switzerland.

Received: 14 September 2021 Accepted: 6 May 2022

Published online: 18 May 2022

References

- Maenner MJ, Shaw KA, Baio J, Washington A, Patrick M, DiRienzo M, et al. Prevalence of Autism spectrum disorder among children aged 8 years—Autism and developmental disabilities monitoring network, 11 sites, United States, 2016. *MMWR Surveill Summ*. 2020;69(4):1–12.
- Lord C, Brugha TS, Charman T, Cusack J, Dumas G, Frazier T, et al. Autism spectrum disorder. *Nat Rev Dis Primer*. 2020;6(1):1–23.
- Masi A, DeMayo MM, Glozier N, Guastella AJ. An overview of Autism spectrum disorder, heterogeneity and treatment options. *Neurosci Bull*. 2017;33(2):183–93.
- Kang E, Keifer CM, Levy EJ, Foss-Feig JH, McPartland JC, Lerner MD. Atypicality of the N170 event-related potential in Autism spectrum disorder: a meta-analysis. *Biol Psychiatry Cogn Neurosci Neuroimaging*. 2018;3(8):657–66.
- Cooke E. Letter of support for N170 ERP as a prognostic biomarker for adaptive social functioning and its potential to stratify study populations in people with Autism spectrum disorders (ASD) without intellectual disability. 2020. Available from: https://www.ema.europa.eu/en/documents/other/letter-support-n170-erp-prognostic-biomarker-adaptive-social-functioning-its-potential-stratify_en.pdf
- Pereida E, Quiroga RQ, Bhattacharya J. Nonlinear multivariate analysis of neurophysiological signals. *Prog Neurobiol*. 2005;77(1):1–37.
- Schnitzler A, Gross J. Normal and pathological oscillatory communication in the brain. *Nat Rev Neurosci*. 2005;6(4):285–96.
- Wang J, Barstein J, Ethridge LE, Mosconi MW, Takarae Y, Sweeney JA. Resting state EEG abnormalities in Autism spectrum disorders. *J Neurodev Disord*. 2013;5(1):24.
- Chan AS, Leung WWM. Differentiating autistic children with quantitative encephalography: a 3-month longitudinal study. *J Child Neurol*. 2006;21(5):391–9.
- Cornew L, Roberts TPL, Blaskey L, Edgar JC. Resting-state oscillatory activity in Autism spectrum disorders. *J Autism Dev Disord*. 2012;42(9):1884–94.
- Sutton SK, Burnette CP, Mundy PC, Meyer J, Vaughan A, Sanders C, et al. Resting cortical brain activity and social behavior in higher functioning children with Autism. *J Child Psychol Psychiatry*. 2005;46(2):211–22.
- Elhabashy H, Raafat O, Afifi L, Raafat H, Abdullah K. Quantitative EEG in autistic children. *Egypt J Neurol Psychiatry Neurosurg*. 2015;52(3):176.
- Sheikhani A, Behnam H, Mohammadi MR, Noroozian M, Mohammadi M. Detection of abnormalities for diagnosing of children with Autism disorders using of quantitative electroencephalography analysis. *J Med Syst*. 2012;36(2):957–63.
- Takagaki K, Russell J, Lippert MT, Motamedi GK. Development of the posterior basic rhythm in children with autism. *Clin Neurophysiol*. 2015;126(2):297–303.
- Coben R, Clarke AR, Hudspeth W, Barry RJ. EEG power and coherence in autistic spectrum disorder. *Clin Neurophysiol*. 2008;119(5):1002–9.
- Orehkova EV, Elsabbagh M, Jones EJ, Dawson G, Charman T, Johnson MH, et al. EEG hyper-connectivity in high-risk infants is associated with later autism. *J Neurodev Disord*. 2014;6(1):40.
- O'Reilly C, Lewis JD, Elsabbagh M. Is functional brain connectivity atypical in autism. A systematic review of EEG and MEG studies. *PLoS ONE*. 2017;12(5):e0175870.

18. Takahashi T, Yamanishi T, Nobukawa S, Kasakawa S, Yoshimura Y, Hiraishi H, et al. Band-specific atypical functional connectivity pattern in childhood autism spectrum disorder. *Clin Neurophysiol*. 2017;128(8):1457–65.
19. Vakorin VA, Doesburg SM, Leung RC, Vogan VM, Anagnostou E, Taylor MJ. Developmental changes in neuromagnetic rhythms and network synchrony in autism. *Ann Neurol*. 2017;81(2):199–211.
20. Wang J, Wang X, Wang X, Zhang H, Zhou Y, Chen L, et al. Increased EEG coherence in long-distance and short-distance connectivity in children with autism spectrum disorders. *Brain Behav*. 2020;10(10):e01796.
21. Charman T, Loth E, Tillmann J, Crawley D, Wooldridge C, Goyard D, et al. The EU-AIMS longitudinal European Autism Project (LEAP): clinical characterisation. *Mol Autism*. 2017;23(8):27.
22. Loth E, Charman T, Mason L, Tillmann J, Jones E, Wooldridge C, et al. The EU-AIMS longitudinal European Autism Project (LEAP): design and methodologies to identify and validate stratification biomarkers for autism spectrum disorders. *Mol Autism*. 2017;23(8):24.
23. Muthukumaraswamy S. High-frequency brain activity and muscle artifacts in MEG/EEG: a review and recommendations. *Front Hum Neurosci*. 2013. <https://doi.org/10.3389/fnhum.2013.00138/full>.
24. Hyvärinen A, Oja E. Independent component analysis: algorithms and applications. *Neural Netw*. 2000;13(4):411–30.
25. Lodder SS, van Putten MJAM. Automated EEG analysis: characterizing the posterior dominant rhythm. *J Neurosci Methods*. 2011;200(1):86–93.
26. Holiga S, Hipp JF, Chatham CH, Garcés P, Spooren W, D'Ardhuy XL, et al. Patients with autism spectrum disorders display reproducible functional connectivity alterations. *Sci Transl Med*. 2019;11(481):eaat9223.
27. Penny WD, Friston KJ, Ashburner JT, Kiebel SJ, Nichols TE. Statistical parametric mapping: the analysis of functional brain images. Elsevier; 2011.
28. Oostenveld R, Fries P, Maris E, Schoffelen J-M. FieldTrip: open source software for advanced analysis of MEG, EEG, and invasive electrophysiological data. *Comput Intell Neurosci*. 2011;2011(1):9.
29. Gabriel S, Lau RW, Gabriel C. The dielectric properties of biological tissues: II. Measurements in the frequency range 10 Hz to 20 GHz. *Phys Med Biol*. 1996;41(11):2251.
30. McCann H, Pisano G, Beltrachini L. Variation in reported human head tissue electrical conductivity values. *Brain Topogr*. 2019;32(5):825–58.
31. Birot G, Spinelli L, Vulliémot S, Mégevand P, Brunet D, Seeck M, et al. Head model and electrical source imaging: a study of 38 epileptic patients. *NeuroImage Clin*. 2014;1(5):77–83.
32. Vorwerk J, Oostenveld R, Piastra MC, Magyari L, Wolters CH. The FieldTrip-SimBio pipeline for EEG forward solutions. *Biomed Eng Online*. 2018;17(1):37.
33. Veen BDV, Drongelen WV, Yuchtman M, Suzuki A. Localization of brain electrical activity via linearly constrained minimum variance spatial filtering. *IEEE Trans Biomed Eng*. 1997;44(9):867–80.
34. Sekihara K, Sahani M, Nagarajan SS. Localization bias and spatial resolution of adaptive and non-adaptive spatial filters for MEG source reconstruction. *Neuroimage*. 2005;25(4):1056–67.
35. Hipp JF, Hawellek DJ, Corbetta M, Siegel M, Engel AK. Large-scale cortical correlation structure of spontaneous oscillatory activity. *Nat Neurosci*. 2012;15(6):884–90.
36. Vinck M, Oostenveld R, van Wingerden M, Battaglia F, Pennartz CMA. An improved index of phase-synchronization for electrophysiological data in the presence of volume-conduction, noise and sample-size bias. *Neuroimage*. 2011;55(4):1548–65.
37. Nolte G, Bai O, Wheaton L, Mari Z, Vorbach S, Hallett M. Identifying true brain interaction from EEG data using the imaginary part of coherency. *Clin Neurophysiol*. 2004;115(10):2292–307.
38. Spence JR, Stanley DJ. Prediction Interval: what to expect when you're expecting ... a replication. *PLoS ONE*. 2016;11(9):e0162874.
39. Pinheiro JC, Bates DM. Mixed-effects models in S and S-PLUS. New York: Springer; 2000.
40. Luke SG. Evaluating significance in linear mixed-effects models in R. *Behav Res Methods*. 2017;49(4):1494–502.
41. Nichols TE, Holmes AP. Nonparametric permutation tests for functional neuroimaging: a primer with examples. *Hum Brain Mapp*. 2002;15(1):1–25.
42. Hastie T, Tibshirani R, Friedman J. The elements of statistical learning: data mining, inference, and prediction. 2nd ed. New York: Springer; 2009.
43. Abraham A, Pedregosa F, Eickenberg M, Gervais P, Mueller A, Kossaifi J, et al. Machine learning for neuroimaging with scikit-learn. *Front Neuroinformatics*. 2014. <https://doi.org/10.3389/fninf.2014.00014/full>.
44. Abraham A, Milham MP, Di Martino A, Craddock RC, Samaras D, Thirion B, et al. Deriving reproducible biomarkers from multi-site resting-state data: an Autism-based example. *Neuroimage*. 2017;15(147):736–45.
45. Plitt M, Barnes KA, Wallace GL, Kenworthy L, Martin A. Resting-state functional connectivity predicts longitudinal change in autistic traits and adaptive functioning in autism. *Proc Natl Acad Sci U S A*. 2015;112(48):E6699–7006.
46. Schouten TM, Koini M, de Vos F, Seiler S, de Rooij M, Lechner A, et al. Individual classification of Alzheimer's disease with diffusion magnetic resonance imaging. *Neuroimage*. 2017;152:476–81.
47. Ball G, Aljabar P, Arichi T, Tusor N, Cox D, Merchant N, et al. Machine-learning to characterise neonatal functional connectivity in the preterm brain. *Neuroimage*. 2016;1(124):267–75.
48. Moghim N, Corne DW. Predicting epileptic seizures in advance. *PLoS ONE*. 2014;9(6):e99334.
49. Varoquaux G, Raamana PR, Engemann DA, Hoyos-Idrobo A, Schwartz Y, Thirion B. Assessing and tuning brain decoders: cross-validation, caveats, and guidelines. *Neuroimage*. 2017;15(145):166–79.
50. Risi S, Lord C, Gotham K, Corsello C, Chrysler C, Szatmari P, et al. Combining information from multiple sources in the diagnosis of autism spectrum disorders. *J Am Acad Child Adolesc Psychiatry*. 2006;45(9):1094–103.
51. Chiang AKI, Rennie CJ, Robinson PA, van Albada SJ, Kerr CC. Age trends and sex differences of alpha rhythms including split alpha peaks. *Clin Neurophysiol*. 2011;122(8):1505–17.
52. Gasser T, Verleger R, Bächer P, Sroka L. Development of the EEG of school-age children and adolescents. I. Analysis of band power. *Electroencephalogr Clin Neurophysiol*. 1988;69(2):91–9.
53. Schäfer CB, Morgan BR, Ye AX, Taylor MJ, Doesburg SM. Oscillations, networks, and their development: MEG connectivity changes with age. *Hum Brain Mapp*. 2014;35(10):5249–61.
54. Somsen RJM, van't Klooster BJ, van der Molen MW, van Leeuwen HMP, Licht R. Growth spurts in brain maturation during middle childhood as indexed by EEG power spectra. *Biol Psychol*. 1997;44(3):187–209.
55. Duffy FH, Shankardass A, McAnulty GB, Als H. The relationship of Asperger's syndrome to autism: a preliminary EEG coherence study. *BMC Med*. 2013;11:175.
56. Duffy FH, Als H. A stable pattern of EEG spectral coherence distinguishes children with autism from neuro-typical controls—a large case control study. *BMC Med*. 2012;10:64.
57. Uddin LQ, Supekar K, Menon V. Reconceptualizing functional brain connectivity in autism from a developmental perspective. *Front Hum Neurosci*. 2013;7:458.
58. Picci G, Gotts SJ, Scherf KS. A theoretical rut: revisiting and critically evaluating the generalized under/over-connectivity hypothesis of autism. *Dev Sci*. 2016;19(4):524–49.
59. Rane P, Cochran D, Hodge SM, Haselgrove C, Kennedy D, Frazier JA. Connectivity in Autism: a review of MRI connectivity studies. *Harv Rev Psychiatry*. 2015;23(4):223–44.
60. Nentwich M, Ai L, Madsen J, Telesford QK, Haufe S, Milham MP, et al. Functional connectivity of EEG is subject-specific, associated with phenotype, and different from fMRI. *Neuroimage*. 2020;1(218): 117001.
61. Hipp JF, Siegel M. BOLD fMRI correlation reflects frequency-specific neuronal correlation. *Curr Biol*. 2015;25(10):1368–74.
62. Edgar JC, Dipiero M, McBride E, Green HL, Berman J, Ku M, et al. Abnormal maturation of the resting-state peak alpha frequency in children with autism spectrum disorder. *Hum Brain Mapp*. 2019;40(11):3288–98.
63. Obermeyer Z, Emanuel EJ. Predicting the future — big data, machine learning, and clinical medicine. *N Engl J Med*. 2016;375(13):1216–9.
64. van der Ploeg T, Austin PC, Steyerberg EW. Modern modelling techniques are data hungry: a simulation study for predicting dichotomous endpoints. *BMC Med Res Methodol*. 2014;14(1):137.
65. Steyerberg E. Clinical prediction models—a practical approach to development, validation, and updating. 2nd ed. Springer; 2019.
66. van Smeden M, Moons KG, de Groot JA, Collins GS, Altman DG, Eijkemans MJ, et al. Sample size for binary logistic prediction models: Beyond events per variable criteria. *Stat Methods Med Res*. 2019;28(8):2455–74.
67. Amaral DG, Schumann CM, Nordahl CW. Neuroanatomy of autism. *Trends Neurosci*. 2008;31(3):137–45.

68. Loth E, Spooren W, Ham LM, Isaac MB, Auriche-Benichou C, Banaschewski T, et al. Identification and validation of biomarkers for autism spectrum disorders. *Nat Rev Drug Discov*. 2016;15(1):70–3.
69. Easson AK, Fatima Z, McIntosh AR. Functional connectivity-based subtypes of individuals with and without autism spectrum disorder. *Netw Neurosci*. 2018;3(2):344–62.
70. Lombardo MV, Lai M-C, Auyeung B, Holt RJ, Allison C, Smith P, et al. Unsupervised data-driven stratification of mentalizing heterogeneity in autism. *Sci Rep*. 2016;6(1):35333.
71. Wolfers T, Floris DL, Dinga R, van Rooij D, Isakoglou C, Kia SM, et al. From pattern classification to stratification: towards conceptualizing the heterogeneity of Autism spectrum disorder. *Neurosci Biobehav Rev*. 2019;1(104):240–54.
72. Byrge L, Dubois J, Tyska JM, Adolphs R, Kennedy DP. Idiosyncratic brain activation patterns are associated with poor social comprehension in Autism. *J Neurosci*. 2015;35(14):5837–50.
73. Hahamy A, Behrmann M, Malach R. The idiosyncratic brain: distortion of spontaneous connectivity patterns in autism spectrum disorder. *Nat Neurosci*. 2015;18(2):302–9.
74. Nunes AS, Peatfield N, Vakorin V, Doesburg SM. Idiosyncratic organization of cortical networks in autism spectrum disorder. *Neuroimage*. 2019;15(190):182–90.
75. Pegado F, Hendriks MHA, Amelynck S, Daniels N, Steyaert J, Boets B, et al. Adults with high functioning autism display idiosyncratic behavioral patterns, neural representations and connectivity of the 'Voice Area' while judging the appropriateness of emotional vocal reactions. *Cortex*. 2020;1(125):90–108.
76. Jones E, Mason L, Moessnang C, Chatham CH, Ham L, Tillmann J, Dumas G, et al. The N170 face-sensitive brain response: toward a stratification biomarker for ASD. *INSAR* 2021.
77. De Stefano LA, Schmitt LM, White SP, Mosconi MW, Sweeney JA, Ethridge LE. Developmental effects on auditory neural oscillatory synchronization abnormalities in autism spectrum disorder. *Front Integr Neurosci*. 2019. <https://doi.org/10.3389/fnint.2019.00034/full>.
78. Freyberg J, Robertson CE, Baron-Cohen S. Reduced perceptual exclusivity during object and grating rivalry in autism. *J Vis*. 2015;15(13):11–11.
79. Vettori S, Dzhelyova M, Van der Donck S, Jacques C, Van Wesemael T, Steyaert J, et al. Combined frequency-tagging EEG and eye tracking reveal reduced social bias in boys with autism spectrum disorder. *Cortex*. 2020;1(125):135–48.
80. DiStefano C, Gulsrud A, Huberty S, Kasari C, Cook E, Reiter LT, et al. Identification of a distinct developmental and behavioral profile in children with Dup15q syndrome. *J Neurodev Disord*. 2016;8(1):19.
81. Percy AK. Rett syndrome: exploring the Autism Link. *Arch Neurol*. 2011;68(8):985–9.
82. Wilkinson CL, Nelson CA. Increased aperiodic gamma power in young boys with Fragile X syndrome is associated with better language ability. *Mol Autism*. 2021;12(1):17.

Publisher's Note

Springer Nature remains neutral with regard to jurisdictional claims in published maps and institutional affiliations.

Ready to submit your research? Choose BMC and benefit from:

- fast, convenient online submission
- thorough peer review by experienced researchers in your field
- rapid publication on acceptance
- support for research data, including large and complex data types
- gold Open Access which fosters wider collaboration and increased citations
- maximum visibility for your research: over 100M website views per year

At BMC, research is always in progress.

Learn more biomedcentral.com/submissions

